Dalton Transactions

PAPER

Cite this: *Dalton Trans.*, 2017, **46**, 9895

Environmentally benign dry-gel conversions of Zr-based UiO metal–organic frameworks with high yield and the possibility of solvent re-use†

Serkan Gökpinar, Tatyana Diment and Christoph Janiak *

Received 11th May 2017,
Accepted 30th June 2017

DOI: 10.1039/c7dt01717k

rsc.li/dalton

Herein we report an alternative synthesis method for Zr-based UiO metal–organic frameworks (MOFs), namely dry-gel conversion (DGC). It was possible to synthesize nano- to microsized UiO-66, UiO-66-NH_2 and UiO-67 with high crystallinity, high surface area and increased yield using only one-sixth or less of the solvent volume compared to the solution synthesis on the same scale. Additionally, it is shown that solvent re-use is possible over at least five synthesis runs making the DGC method an ecological and extremely solvent-economical route to obtain Zr-based UiO-MOFs with reproducible results.

Introduction

Metal–organic frameworks (MOFs) are potentially porous materials consisting of metal ions or metal clusters connected by organic ligands[1,2] and are actively investigated towards various applications.[3–6]

Among the most intensively studied MOFs is the isoreticular UiO-series, especially UiO-66 (UiO = University in Oslo),[7–9] which was first synthesized by Lillerud and co-workers.[10] Zirconium(IV)-based UiO-MOFs have a $\{Zr_6O_4(OH)_4\}$- or $\{Zr_6O_4(OH)_4(-CO_2)_{12}\}$-SBU which is 12 coordinated by the linker molecules.[10] UiO-66 has benzene-1,4-dicarboxylate linkers (BDC), while UiO-67 contains biphenyl-4,4′-dicarboxylate (BPDC) linkers.[10] The SBU is an octahedral cluster of six edge-sharing ZrO_8 square-antiprisms, which is connected to 12 neighboring SBUs in a face-centered cubic (fcc) packing arrangement (see Fig. S1 in the ESI†). The properties of these UiO-MOFs are interesting for gas storage,[11] separation,[12] water sorption,[8,13] sensing[14] and catalysis.[15]

Much research is currently done to optimize the synthesis techniques of MOFs also in an environmentally and economically advantageous way.[16] Goals are to find synthesis routes to decrease the reaction time, temperature or solvent consumption and to avoid the use of HF or acidic fluoride solutions.[17,18] Ultrasound can be applied for rapid and low-temperature syntheses, for example for MIL-53(Fe),[19] HKUST-1[20] and MOF-5.[21] Mechanochemical methods can be realized without any solvent and are known, for example, for MIL-101 (Cr)[22] and UiO-66.[23] Alternatively, microwave heating-induced synthesis can be used to obtain UiO-66.[24] Advantages like fast crystallization and phase selectivity can be achieved. A recent alternative synthesis method for MOFs is dry-gel conversion (DGC). In Fig. 1, the working principle of the DGC method is illustrated. A small amount of solvent is placed at the bottom of a Teflon container and the solid starting materials are placed up in the head on a sieve or porous support.[25] Consequently, the physical separation of the solvent and reactant mixture is achieved. From this separation results one of the big advantages of DGC, namely after the reaction, the solvent can be recovered largely uncontaminated and can be used for further reaction runs. This possibility offers an easy solvent re-use and can be interesting for industrial applications. The advantages of DGC are strongly reduced consumption of the solvent with no production of the mother liquor which needs to be disposed,[26] high product yields,[27,28] reduced reactor size and the possibility of continuous production.[25]

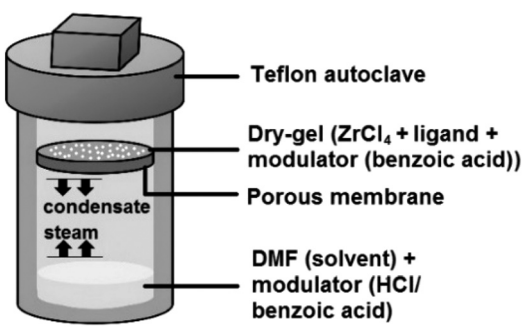

Fig. 1 Schematic drawing of the reactor setup for DGC with starting materials for the synthesis of UiOs.

Institut für Anorganische Chemie und Strukturchemie, Heinrich-Heine-Universität Düsseldorf, 40204 Düsseldorf, Germany. E-mail: janiak@uni-duesseldorf.de

† Electronic supplementary information (ESI) available: Synthesis and characterization details, TGA and defect calculations, PXRD patterns, pore size distributions, SEM images and reproducibility data. See DOI: 10.1039/c7dt01717k

For the synthesis of zeolites, steam-assisted DGC methods are used very often,[22,24] but so far there have been only a few reports about the DGC synthesis of MOFs.[29–31] Shi *et al.* synthesized zeolitic imidazolate framework (ZIF) materials (ZIF-8 and ZIF-67) through DGC by replacing dimethylformamide (DMF) with water as the solvent.[32] The DGC synthesis of MIL-100(Fe) without adding hydrofluoric acid (HF) to the reaction mixture was established by Ahmed *et al.*[33] Kim *et al.* reported the DGC synthesis of MIL-101(Cr) using water as the solvent and HF acid as an additive.[34] Recently, Tan *et al.* used DGC for the synthesis of magnetically responsive HKUST-1/Fe_3O_4 composites.[35]

Experimental

Materials

All reagents were used as received. Terephthalic acid H_2BDC, biphenyl-4,4′-dicarboxylic acid, H_2BPDC, ethanol and hydrochloric acid 37% (HCl) were purchased from Sigma Aldrich. *N*,*N*′-Dimethylformamide (DMF) was obtained from Fischer Chemicals. 2-Aminoterephthalic acid (NH_2-H_2BDC) and anhydrous $ZrCl_4$ were purchased from Alfa Aesar. Benzoic acid (BA) was purchased from Riedel de Haen. Alternatively, the use of benzoic acid in technical grade is possible.

Instrumentation

Powder X-ray diffraction (PXRD) patterns were obtained at ambient temperature on a Bruker D2 phaser (300 W, 30 kV, 10 mA) using Cu-Kα radiation (λ = 1.54182 Å) between 5° < 2Θ < 50° with a scanning rate of 0.0125° s^{-1}. The diffractograms were obtained on a flat "low background sample holder", in which at low angle the beam spot is strongly broadened so that only a fraction of the reflected radiation reaches the detector, hence the low relative intensities measured at 2Θ < 7°. The analyses of the diffractograms were carried out with "Match 3.11" software. Thermogravimetric analysis (TGA) was performed with a Netzsch TG209 F3 Tarsus instrument. Samples were placed in alumina pans and heated at a rate of 5 °C min^{-1} from 25 to 700 °C under a nitrogen atmosphere. Nitrogen (purity 99.9990%) physisorption isotherms were obtained on a Nova 4000e from Quantachrome at 77 K. Before obtaining the isotherms, the products were transferred into glass tubes capped with septa, which were weighed before. These tubes were attached to the corresponding degassing port of the sorption analyzer, degassed under vacuum at 120 °C for 3 h, weighed again and then transferred to the analysis port of the sorption analyzer. BET surface areas were calculated from the nitrogen adsorption isotherms in the p/p_0 range of 0.005–0.05. Total pore volumes were calculated from the nitrogen sorption isotherm at p/p_0 = 0.95. DFT calculations for the pore size distribution curves were carried out with the native 'NovaWin 11.03' software using the 'N_2 at 77 K on carbon, slit pore, NLDFT equilibrium' model. SEM images were recorded with a Jeol JSM-6510LV QSEM advanced electron microscope with a LaB_6 cathode at 5–20 keV. The microscope was equipped with a Bruker Xflash 410 silicon drift detector.

DGC synthesis of UiOs

For UiO-66-BA, $ZrCl_4$ (60 mg, 0.26 mmol), H_2BDC (44 mg, 0.26 mmol) and benzoic acid (0.2 g, 1.64 mmol) were mixed, ground and placed in a DGC sieve. A small amount (typically 2.5 mL) of DMF solvent was placed at the bottom of a 15 mL Teflon container and benzoic acid (1.4 g, 11.46 mmol) was added to the solvent. The DGC sieve was placed above the solvent mixture and the Teflon container was capped. The Teflon container was sealed in a stainless steel autoclave, and allowed to react at 120 °C for 24 h in a preheated oven. After cooling, the obtained as-synthesized product was left to soak in DMF (2 × 5 mL) and ethanol (5 mL) for 3 d. The solution was exchanged every 24 h. After 3 d of soaking, the solids were centrifuged and dried under vacuum. In the case of HCl modulation, only 0.5 mL of 37% aqueous HCl was added to the solvent. For the synthesis of UiO-66-NH_2, H_2BDC was replaced by NH_2-H_2BDC, and for UiO-67, H_2BPDC was used. More detailed information on the syntheses, workup procedure and characterization is given in the ESI (section S3†).

Results and discussion

Synthesis and characterisation

To the best of our knowledge, the synthesis of Zr-based UiO-MOFs by the DGC method has not been reported so far. Herein, we present a facile synthesis of UiO-MOFs using the DGC method. In the present study, UiO-66, UiO-66-NH_2 and UiO-67 were synthesized from $ZrCl_4$, H_2BDC, NH_2-H_2BDC or H_2BPDC, respectively, with DMF and a modulator (BA or HCl).

The modulator BA was chosen for several reasons: BA modulation delivers product advantages for UiOs which are discussed by Atzori *et al.*[36] They proved that monocarboxylic acid modulation supports the formation of "missing-cluster defects" whose charge and coordination deficiencies are compensated for by modulator ligands.[36] Important for DGC, BA modulation delivered products with stable and thick consistency. Also, BA in the solvent at the bottom of the container has an important role. If we do not use a solvent–modulator mixture a large part, if not all of the MOF product, is washed into the solvent (section S3 in the ESI†). Hence, the solvent cannot be re-used.

For batch sizes of 0.26 mmol of $ZrCl_4$ starting material, the DGC uses only 2.5 mL of DMF, while the standard solvothermal solution synthesis requires up to 15 mL of DMF solvent (see section S4 in the ESI†). Larger amounts of the solvent are also used in the washing procedure of the UiO products from solution synthesis.[37] In the case of benzoic acid modulated UiO, 112.5 mL of MeOH were used, while the DGC method used only 10 mL of DMF and 5 mL of EtOH for comparative yields of products. Both DGC and solution synthesis yield nearly the same amount of UiO products (83 mg from DGC and 80 mg from solution synthesis) for identical

amounts of the starting material (0.26 mmol of $ZrCl_4$) (see sections S3 and S4 in the ESI†). Several synthesis routes for UiO-66 are listed by Hu and Zhao.[38] A detailed comparison of UiO-66 through DGC and solution synthesis is given in Table S4 in the ESI.†

Fig. 2 shows the powder X-ray diffraction (PXRD) patterns of the obtained UiO products which verify their crystallinity and phase purity by positive matching with the simulated patterns. The experimental PXRD patterns contain a broad peak in the 2θ range of *ca.* 5–7°. This peak is not seen in the simulation of the UiO-66 phase, hence, it cannot be attributed to the UiO-66 phase. In the work of Shearer *et al.*, this "broad peak" was found in the 2θ range of 4–6° and assigned to **reo** nanoregions, where the **reo** phase can be thought of as UiO-66 with one-quarter of its clusters missing.[9] The slight shift in the 2θ range of this broad peak in the work of Shearer *et al.* may be due to the fact that their PXRD samples were activated (*i.e.*, desolvated) prior to the measurement, while our PXRD samples were measured only after a short activation time of 2 h at 120 °C. In our PXRD patterns, the broad peak is most prominent in the UiO-66-BA samples (see Fig. 2 and Fig. S6 and S8 in the ESI†).

Fig. 3 depicts the N_2 adsorption–desorption isotherms of the obtained UiO-MOFs with different modulators. The resulting BET surface areas and pore volumes are summarized in Table 1. The BET surface areas of UiOs from DGC are highly comparable to the results from the solution synthesis in the literature. The BET surface area of UiO-66 depends on the modulator such that HCl yielded a higher surface area than BA. On the other hand, BA modulated approaches deliver higher yields. The pore size distributions of selected UiOs are compared in the ESI (Fig. S7†). All obtained results are reproducible. Only weak fluctuations of the surface area and yield are observed in the first synthesis runs for different batches. This reproducibility of DGC for UiO-66-BA without the re-use of the solvent is shown in the ESI (Fig. S9†).

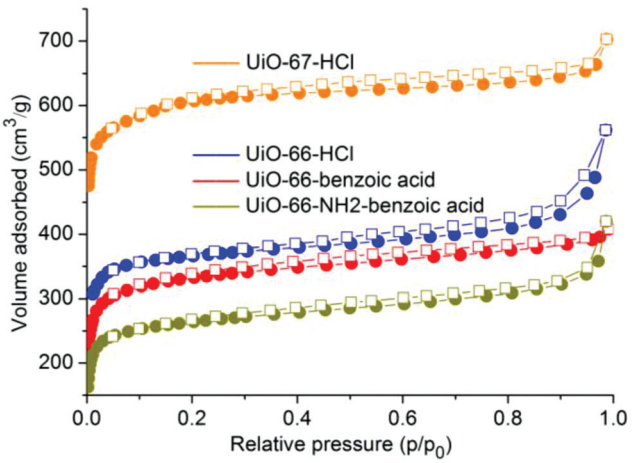

Fig. 3 N_2 sorption isotherms of UiO-66-NH_2-BA, UiO-66-BA, UiO-66-HCl and UiO-67-HCl synthesized through DGC. Filled symbols, adsorption; empty symbols, desorption.

Table 1 Results of DGC synthesis of UiO-66, UiO-66-NH_2 and UiO-67 with different modulators

MOF and modulator	BET surface area ($m^2\ g^{-1}$)	BET surface Lit.[a] ($m^2\ g^{-1}$)	Pore volume ($cm^3\ g^{-1}$)	Yield (mg)
UiO-66-BA	1242	1032 [8]–1450 [40]	0.550	83
UiO-66-HCl	1461		0.689	65
UiO-66-NH_2-BA	1023	1200 (HCl)[7]	0.485	93
UiO-67-HCl	2369	2500 [7]	0.911	82

[a] Results from standard solution synthesis in the literature.

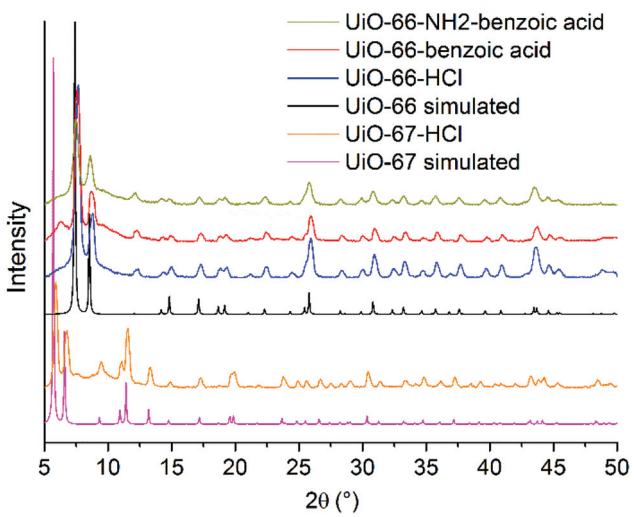

Fig. 2 PXRD patterns of simulated UiO-67, synthesized UiO-67-HCl, simulated UiO-66, synthesized UiO-66-HCl, UiO-66-BA and UiO-66-NH_2-BA from DGC. 'Benzoic acid' and 'HCl' refer to the used modulator. The simulated pattern of UiO-66 calculated from CSD-Refcode RUBTAK02,[39] and the simulated pattern of UiO-67 calculated from WIZMAV03.[40] For the four experimental PXRD patterns, we have also collected the diffractograms down to 2θ = 2° without observing additional peaks below 2θ = 5° (see Fig. S6 in the ESI†).

Nanocrystals were obtained for MFI type ferrisilicate zeolites through the DGC method.[41] No such observation on nanocrystals through DGC has yet been made for MOFs. Here we note that the primary particle size of UiO-66-HCl from DGC is between ~90 and 200 nm as illustrated by scanning electron microscopy images in Fig. 4. In comparison, Pullen *et al.* obtained UiO-66 crystals with a particle size ranging from ~200 to 500 nm through solution synthesis.[37] The DGC UiO-66-NH_2-BA particles vary from 200 to 500 nm. The primary particles of DGC UiO-67-HCl are around 500 nm, which are smaller than expected. Nik *et al.* obtained 1 μm-sized UiO-67 particles.[42] The selected SEM images are shown in Fig. 4. Further images are illustrated in Fig. S8 in the ESI.†

Characterization of defects

In TGA, three weight losses are observed. Firstly, solvent residues are removed in a temperature interval between 25 and 100 °C. Secondly, the removal of monocarboxylate ligands (BA)

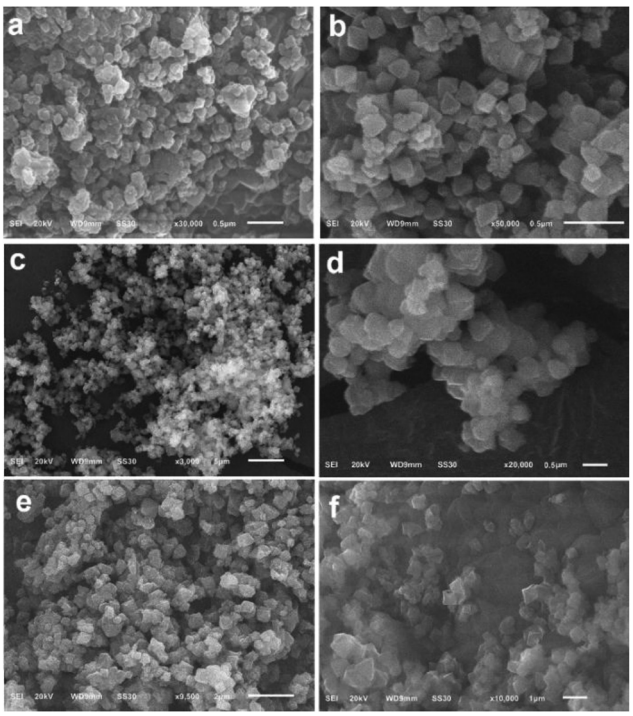

Fig. 4 SEM image of UiO-66-HCl (a and b), UiO-66-NH_2-BA (c and d) and UiO-67-HCl (e and f). Scale bar is 0.5 μm for a, b and d; 5 μm for c; 2 μm for e; 1 μm for f.

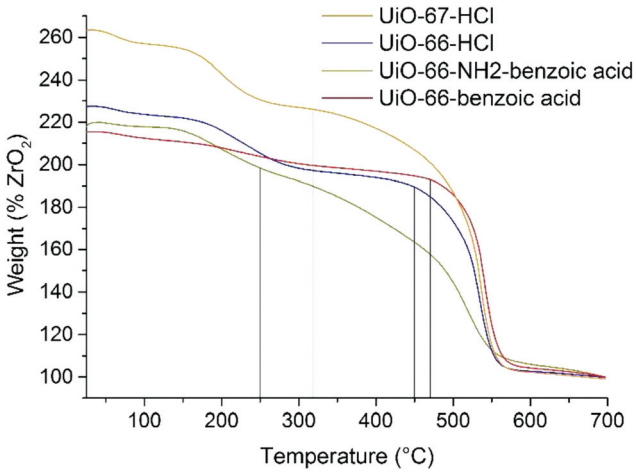

Fig. 5 TGA of UiO-66-NH_2-BA, UiO-66-BA, UiO-66-HCl and UiO-67-HCl synthesized through DGC (end weight normalized to 100%; the used area for $W_{Exp.Plat}$ is marked).

Table 2 Determination of defects from TGA

	Number of defects per SBU (x – *cf.* ESI)[a]	Molecular formula $Zr_6O_{6+x}(BDC)_{6-x}$ [b]	Exp. molecular weight (g mol^{-1})
UiO-66-HCl	1.6	$Zr_6O_{7.6}(BDC)_{4.4}$	1397.48
UiO-66-BA	1.4	$Zr_6O_{7.4}(BDC)_{4.6}$	1427.10
UiO-66-NH_2-BA	1.6	$Zr_6O_{7.6}(NH_2\text{-}BDC)_{4.4}$	1463.81
UiO-67-HCl	1.9	$Zr_6O_{7.9}(BPDC)_{4.1}$	1663.39

[a] The used experimental weights $W_{Exp.Plat}$ and the mathematical calculations to derive at x are presented in the ESI (section S2). Values are rounded to one decimal digit, taking into account the experimental accuracy. [b] The determination of defects from TGA was performed according to the seminal work of Shearer *et al.*[9] where the molecular formula and experimental molecular weight derived therefrom were reported in the same way, that is, without modulator units in place of the missing BDC linkers.

and the dehydroxylation of the $\{Zr_6O_4(OH)_4\}$ SBUs occur.[9] Both weight losses take place in a similar temperature range (*ca.* 180–300 °C),[39] followed by framework decomposition above *ca.* 350–550 °C.[39] Temperature ranges can be shifted depending on the used linker. The analysis of the weight losses allows the determination of linker defects as was shown by Shearer *et al.*[9] The calculation of defects was carried out according to this work.[9] The quantitative analysis of TGA data obtained on UiO MOFs was performed with the assumption that the residue in each TGA experiment is pure ZrO_2. Fig. 5 shows the TGA results of the obtained UiO products, with the residual mass set to 100%. A detailed determination of defects for selected UiO samples is outlined in the ESI (section S2†). The results of thermogravimetric analysis towards the number of defects are summarized in Table 2. The number of defects per SBU varies somewhat. The number of defects per SBU, that is per Zr_6 formula unit was in the range of 1.4 to 1.9 which is in the same range as the number of linker deficiencies reported by Shearer *et al.* for trifluoroacetic and difluoroacetic acid depending on the molar equivalents of the modulator used in the synthesis.[9]

Solvent re-use

The spatial separation of solvent and reaction products in DGC allows the solvent to be recovered largely uncontaminated. Therefore, we also tested the solvent re-use for further reaction runs. For the first run of the DGC synthesis of UiO-66, the solvent DMF was mixed with the modulator BA and placed at the bottom of the Teflon container. The precursor mixture of $ZrCl_4$, H_2BDC and BA was placed on the porous support (*cf.* Fig. 1). When run 1 was completed, the porous support with the reaction products from the head of the container was carefully removed without contaminating the solvent. For run 2, another support containing the freshly prepared precursor mixture was placed in the Teflon container with the same solvent mixture from run 1. This synthesis and workup procedure was repeated at 120 °C for 24 hours over five runs. The results concerning the yield and BET surface area of the UiO-66 products with the re-use of the same 2.5 mL DMF solvent are shown in Fig. 6. BET surface areas vary between 1242 and 936 $m^2\ g^{-1}$. We obtained the yields between 68 and 83 mg per run, while solution synthesis delivered a yield of 80 mg per run. In comparison with the reproducibility of the first synthesis runs (*cf.* Fig. S9 in the ESI†), we observe that upon solvent recycling the surface area and yield vary strongly. Nonetheless, the surface area and yield remain in an acceptable range. Notably, the surface area and yield do not only

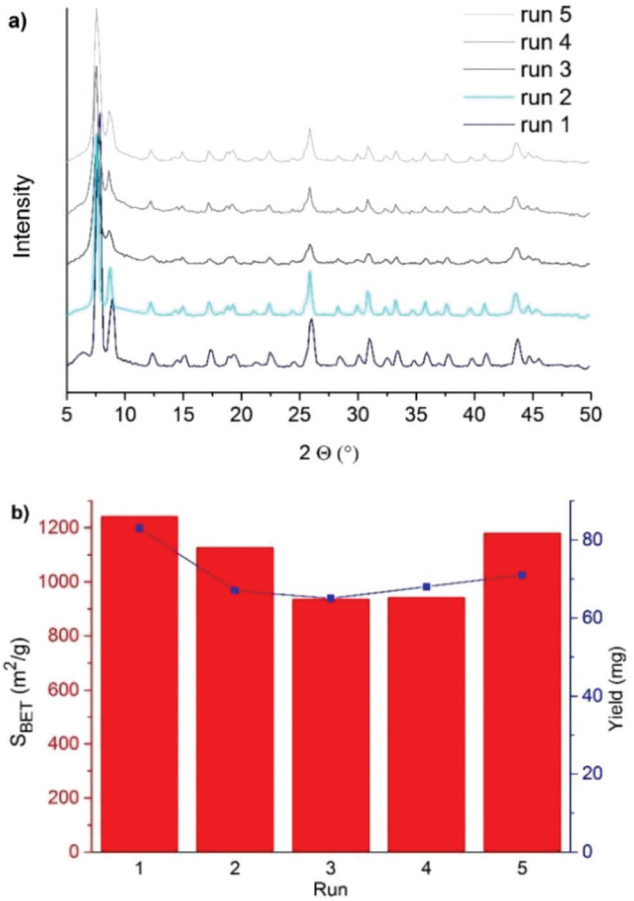

Fig. 6 Results of five DGC runs re-using the same solvent/modulator mixture for UiO-66-BA. (a) Surface area and yield of UiO-66-BA and (b) PXRD patterns of each run.

decrease but also recover from run 3 to run 5. The solvent re-use procedure over five runs was also successfully carried out for the synthesis of UiO-66-NH_2 (see section S9 in the ESI†). More detailed information on the syntheses, workup and characterization is given in the ESI.†

Conclusions

The dry-gel conversion (DGC) of the prototypical MOFs UiO-66, UiO-66-NH_2 and UiO-67 modulated with benzoic acid (BA) or hydrochloric acid (HCl/H_2O) was successful and highly reproducible. BA modulated UiOs were obtained in high yields and as highly stable dry gels; HCl modulated UiOs exhibited higher surface areas than their BA-modulated counterparts. Both modulators give rise to defects in the range of 1.4–1.9 defects per Zr_6-SBU. DGC uses only one-sixth or less of the solvent than the same scale solution synthesis. Additionally, it was proven that a re-use of the solvent over at least five synthesis runs is possible which reduces the needed DMF solvent volume for the total amount of the product even further to 1/30 or less of the solution synthesis.

Conflict of interest

There are no conflicts of interest to declare.

Acknowledgements

The work was supported by the Federal German Ministry of Education and Research (BMBF) under grant# 03SF0492C. We thank Carsten Schlüsener, Sandra Nießing and Dennis Dietrich for the SEM images and Alexa Schmitz for performing TGA.

References

1 H. C. Zhou, J. R. Long and O. M. Yaghi, *Chem. Rev.*, 2012, **112**, 673–674.
2 H. Furukawa, K. E. Cordova, M. O'Keeffe and O. M. Yaghi, *Science*, 2013, **341**, 1230444.
3 C. Janiak and J. K. Vieth, *New J. Chem.*, 2010, **34**, 2366–2388.
4 O. M. Yaghi, M. O'Keeffe, N. W. Ockwig, H. K. Chae, M. Eddaoudi and J. Kim, *Nature*, 2003, **423**, 705–714.
5 M. Eddaoudi, D. B. Moler, H. Li, B. Chen, T. M. Reineke, M. O'Keeffe and O. M. Yaghi, *Acc. Chem. Res.*, 2001, **34**, 319–330.
6 N. W. Ockwig, O. Delgado-Friedrichs, M. O'Keeffe and O. M. Yaghi, *Acc. Chem. Res.*, 2005, **38**, 176–182.
7 M. J. Katz, Z. J. Brown, Y. J. Colón, P. W. Siu, K. A. Scheidt, R. Q. Snurr, J. T. Hupp and O. K. Farha, *Chem. Commun.*, 2013, **49**, 9449–9451.
8 F. Jeremias, V. Lozan, S. K. Henninger and C. Janiak, *Dalton Trans.*, 2013, **42**, 15967–15973.
9 G. C. Shearer, S. Chavan, S. Bordiga, S. Svelle, U. Olsbye and K. P. Lillerud, *Chem. Mater.*, 2016, **28**, 3749–3761.
10 J. H. Cavka, S. Jakobsen, U. Olsbye, N. Guillou, C. Lamberti, S. Bordiga and K. P. Lillerud, *J. Am. Chem. Soc.*, 2008, **130**, 13850–13851.
11 H. Wu, Y. S. Chua, V. Krungleviciute, M. Tyagi, P. Chen, T. Yildirim and W. Zhou, *J. Am. Chem. Soc.*, 2013, **135**, 10525–10532.
12 M. W. Anjum, F. Vermoortele, A. L. Khan, B. Bueken, D. E. De Vos and I. F. J. Vankelecom, *ACS Appl. Mater. Interfaces*, 2015, **7**, 25193–25201.
13 F. Jeremias, D. Fröhlich, C. Janiak and S. Henninger, *New J. Chem.*, 2014, **38**, 1846–1852.
14 A. Shahat, H. M. A. Hassan and H. M. E. Azzazy, *Anal. Chim. Acta*, 2013, **793**, 90–98.
15 F. Vermoortele, B. Bueken, G. Le Bars, B. Van de Voorde, M. Vandichel, K. Houthoofd, A. Vimont, M. Daturi, M. Waroquier, V. Van Speybroeck, C. Kirschhock and D. E. De Vos, *J. Am. Chem. Soc.*, 2013, **135**, 11465–11468.
16 N. Stock and S. Biswas, *Chem. Rev.*, 2012, **112**, 933–969.
17 T. Zhao, F. Jeremias, I. Boldog, B. Nguyen, S. K. Henninger and C. Janiak, *Dalton Trans.*, 2015, **44**, 16791–16801.

18 F. Jeremias, S. K. Henninger and C. Janiak, *Dalton Trans.*, 2016, **45**, 8637–8644.
19 E. Haque, N. A. Khan, J. H. Park and S. H. Jhung, *Chem. – Eur. J.*, 2010, **16**, 1046–1052.
20 Z.-Q. Li, L.-G. Qiu, T. Xu, Y. Wu, W. Wang, Z.-Y. Wu and X. Jiang, *Mater. Lett.*, 2009, **63**, 78–80.
21 W.-J. Son, J. Kim, J. Kim and W.-S. Ahn, *Chem. Commun.*, 2008, **47**, 6336–6338.
22 K. Leng, Y. Sun, X. Li, S. Sun and W. Xu, *Cryst. Growth Des.*, 2016, **16**, 1168–1171.
23 K. Uzarevic, T. C. Wang, S.-Y. Moon, A. M. Fidelli, J. T. Hupp, O. K. Farha and T. Friscic, *Chem. Commun.*, 2016, **52**, 2133–2136.
24 Y. Li, Y. Liu, W. Gao, L. Zhang, W. Liu, J. Lu, Z. Wang and Y.-J. Deng, *CrystEngComm*, 2014, **16**, 7037–7042.
25 M. Matsukata, M. Ogura, T. Osaki, P. R. Hari Prasad Rao, M. Nomura and E. Kikuchi, *Top. Catal.*, 1999, **9**, 77–92.
26 N. Yang, M. Yue and Y. Wang, *Prog. Chem.*, 2012, **24**, 253–261.
27 C. S. Cundy and P. A. Cox, *Chem. Rev.*, 2003, **103**, 663–702.
28 S. Goergen, E. Guillon, J. Patarin and L. Rouleau, *Microporous Mesoporous Mater.*, 2009, **126**, 283–290.
29 X. Feng, C. Jia, J. Wang, X. Cao, P. Tang and W. Yuan, *Green Chem.*, 2015, **17**, 3740–3745.
30 C. M. Jia, J. Wang, X. Feng, Q. Lin and W. B. Yuan, *CrystEngComm*, 2014, **16**, 6552–6555.
31 N. D. McNamara and J. C. Hicks, *ACS Appl. Mater. Interfaces*, 2015, **7**, 5338–5346.
32 Q. Shi, Z. F. Chen, Z. W. Song, J. P. Li and J. X. Dong, *Angew. Chem., Int. Ed.*, 2011, **50**, 672–675.
33 I. Ahmed, J. Jeon, N. A. Khan and S. H. Jhung, *Cryst. Growth Des.*, 2012, **12**, 5878–5881.
34 J. Kim, Y. R. Lee and W. S. Ahn, *Chem. Commun.*, 2013, **49**, 7647–7649.
35 P. Tan, X.-Y. Xie, X.-Q. Liu, T. Pan, C. Gu, P.-F. Chen, J.-Y. Zhou, Y. Pan and L.-B. Sun, *J. Hazard. Mater.*, 2017, **321**, 344–352.
36 C. Atzori, G. C. Shearer, L. Maschio, B. Civalleri, F. Bonino, C. Lamberti, S. Svelle, K. P. Lillerud and S. Bordiga, *J. Phys. Chem. C*, 2017, **121**, 9312–9324.
37 S. Pullen, H. Fei, A. Orthaber, S. M. Cohen and S. Ott, *J. Am. Chem. Soc.*, 2013, **135**, 16997–17003.
38 Z. Hu and D. Zhao, *Dalton Trans.*, 2015, **44**, 19018–19040.
39 L. Valenzano, B. Civalleri, S. Chavan, S. Bordiga, M. H. Nilsen, S. Jakobsen, K. P. Lillerud and C. Lamberti, *Chem. Mater.*, 2011, **23**, 1700–1718.
40 O. V. Gutov, M. G. Hevia, E. C. Escudero-Adan and A. Shafir, *Inorg. Chem.*, 2015, **54**, 8396–8400.
41 K. Miyake, Y. Hirota, K. Ono, Y. Uchida, M. Miyamoto and N. Nishiyama, *New J. Chem.*, 2017, **41**, 2235–2240.
42 O. G. Nik, X. Y. Chen and S. Kaliaguine, *J. Membr. Sci.*, 2012, **413–414**, 48–61.